EAGE

ECMOR | 2022

European Conference on the Mathematics of Geological Reservoirs

5-7 SEPTEMBER 2022 I THE HAGUE, THE NETHERLANDS & ONLINE

WWW.ECMOR.ORG

EAGE

Abstract No. 109
Modeling and Optimization of Shallow Geothermal Heat Storage

Øystein Klemetsdal[1] Halvor Møll Nilsen[1] Stein Krogstad[1]
Odd Andersen[1] Eivind Bastesen[2]

[1]Mathematics and Cybernetics, SINTEF Digital
[2]Ruden AS

EAGE

Geothermal energy storage

Typical energy system: strong temporal variations in supply (wind, solar, ...) and/or demand (day/night, summer/winter), with imbalance between supply and demand (Dincer 2000; Barbier 2002; Gallup 2009; Baria et al. 1999)

- Buffer imbalance by storing excess energy underground as hot water
- In this work: energy storage in shallow, fractured subsurface rock formations
  - Circulate hot/cold water through fracture network by means of wells
  - Fractures serve the same purpose as the fins of a conventional heat exchanger
  - Thermal energy used either directly e.g. in greenhouses and for deicing, or extracted using heat pump

Governing equations and discretization

Finite volumes in space, implicit backward Euler in time

$$\boldsymbol{R}_w^{n+1} = \frac{1}{\Delta t^n}(\boldsymbol{M}_w^{n+1} - \boldsymbol{M}_w^n) + \texttt{div}(\boldsymbol{V}_w^{n+1}) - \boldsymbol{Q}_w^{n+1} = \boldsymbol{0}$$

$$\boldsymbol{V}_w = -\texttt{upw}(\boldsymbol{\rho}_w/\boldsymbol{\mu}_w)\boldsymbol{\Theta}[\texttt{grad}(\boldsymbol{p}) - g\texttt{favg}(\boldsymbol{\rho}_w)\texttt{grad}(\boldsymbol{z})]$$

- $\boldsymbol{\Theta}\texttt{grad}$: discrete representation of $\mathbf{K}\nabla$ (linear/nonlinear two-/multipoint, etc.)
  - In this work: linear two-point flux approximation (comparison: Klemetsdal et al. 2020)
  - $\boldsymbol{\Theta}$: vector of interface transmissibilities
- $\texttt{div}$: divergence, $\texttt{upw}$: upwind (single-point here), $\texttt{favg}$: face average

$\boldsymbol{M}$	Mass	$\boldsymbol{V}$	Flux	$\boldsymbol{Q}$	Sources/sinks	g	Gravity
$\boldsymbol{\rho}$	Density	$\boldsymbol{\mu}$	Viscosity	$\boldsymbol{u}$	Internal energy	$\boldsymbol{h}$	Enthalpy
$\boldsymbol{p}$	Pressure	$\boldsymbol{T}$	Temperature	$\boldsymbol{K}$	Permeability	$\boldsymbol{\Lambda}$	Thermal cond.

Governing equations and discretization

EAGE

Finite volumes in space, implicit backward Euler in time

$$\boldsymbol{R}_w^{n+1} = \frac{1}{\Delta t^n}(\boldsymbol{M}_w^{n+1} - \boldsymbol{M}_w^n) + \texttt{div}(\boldsymbol{V}_w^{n+1}) - \boldsymbol{Q}_w^{n+1} = \boldsymbol{0}$$

$$\boldsymbol{V}_w = -\texttt{upw}(\boldsymbol{\rho}_w/\boldsymbol{\mu}_w)\boldsymbol{\Theta}[\texttt{grad}(\boldsymbol{p}) - g\texttt{favg}(\boldsymbol{\rho}_w)\texttt{grad}(\boldsymbol{z})]$$

Conservation of mass

Darcy's law

- $\boldsymbol{\Theta}\texttt{grad}$: discrete representation of $\mathbf{K}\nabla$ (linear/nonlinear two-/multipoint, etc.)
  - In this work: linear two-point flux approximation (comparison: Klemetsdal et al. 2020)
  - $\boldsymbol{\Theta}$: vector of interface transmissibilities
- `div`: divergence, `upw`: upwind (single-point here), `favg`: face average

$\boldsymbol{M}$	Mass	$\boldsymbol{V}$	Flux	$\boldsymbol{Q}$	Sources/sinks	g	Gravity
$\boldsymbol{\rho}$	Density	$\boldsymbol{\mu}$	Viscosity	$\boldsymbol{u}$	Internal energy	$\boldsymbol{h}$	Enthalpy
$\boldsymbol{p}$	Pressure	$\boldsymbol{T}$	Temperature	$\boldsymbol{K}$	Permeability	$\boldsymbol{\Lambda}$	Thermal cond.

Governing equations and discretization

Finite volumes in space, implicit backward Euler in time

$$\boldsymbol{R}_w^{n+1} = \frac{1}{\Delta t^n}(\boldsymbol{M}_w^{n+1} - \boldsymbol{M}_w^n) + \texttt{div}(\boldsymbol{V}_w^{n+1}) - \boldsymbol{Q}_w^{n+1} = \boldsymbol{0}$$

$$\boldsymbol{V}_w = -\texttt{upw}(\boldsymbol{\rho}_w/\boldsymbol{\mu}_w)\boldsymbol{\Theta}[\texttt{grad}(\boldsymbol{p}) - g\texttt{favg}(\boldsymbol{\rho}_w)\texttt{grad}(\boldsymbol{z})]$$

Conservation of mass

Darcy's law

- $\boldsymbol{\Theta}\texttt{grad}$: discrete representation of $\mathbf{K}\nabla$ (linear/nonlinear two-/multipoint, etc.)
  - In this work: linear two-point flux approximation (comparison: Klemetsdal et al. 2020)
  - $\boldsymbol{\Theta}$: vector of interface transmissibilities
- `div`: divergence, `upw`: upwind (single-point here), `favg`: face average

$\boldsymbol{M}$	Mass	$\boldsymbol{V}$	Flux	$\boldsymbol{Q}$	Sources/sinks	g	Gravity
$\boldsymbol{\rho}$	Density	$\boldsymbol{\mu}$	Viscosity	$\boldsymbol{u}$	Internal energy	$\boldsymbol{h}$	Enthalpy
$\boldsymbol{p}$	Pressure	$\boldsymbol{T}$	Temperature	$\boldsymbol{K}$	Permeability	$\boldsymbol{\Lambda}$	Thermal cond.

EAGE

Governing equations and discretization

Finite volumes in space, implicit backward Euler in time

$$\boldsymbol{R}_h^{n+1} = \frac{1}{\Delta t^n}\left([\boldsymbol{M}_w \boldsymbol{u}_w + \boldsymbol{M}_r \boldsymbol{u}_r]^{n+1} - [\boldsymbol{M}_w \boldsymbol{u}_w + \boldsymbol{M}_r \boldsymbol{u}_r]^{n}\right) + \mathtt{div}\left([\boldsymbol{V}_w \boldsymbol{h}_w + \boldsymbol{H}_c]^{n+1}\right) - [\boldsymbol{Q}_w \boldsymbol{h}_w]^{n+1} - \boldsymbol{Q}_h^{n+1} = \boldsymbol{0}$$

$$\boldsymbol{H}_c = -(\boldsymbol{\Theta}_{hw} + \boldsymbol{\Theta}_{hr})\mathtt{grad}(\boldsymbol{T})$$

- Conductive heat flux $\boldsymbol{H}_c$ discretized by two-point method (same as mass flux)
  - $(\boldsymbol{\Theta}_{hw} + \boldsymbol{\Theta}_{hr})\mathtt{grad}$: discrete representation of $(\boldsymbol{\Lambda}_w + \boldsymbol{\Lambda}_r)\nabla$
  - $\boldsymbol{\Theta}_{hw}$, $\boldsymbol{\Theta}_{hr}$: vectors of interface heat transmissibilities

$\boldsymbol{M}$	Mass	$\boldsymbol{V}$	Flux	$\boldsymbol{Q}$	Sources/sinks	g	Gravity
ρ	Density	μ	Viscosity	$\boldsymbol{u}$	Internal energy	$\boldsymbol{h}$	Enthalpy
$\boldsymbol{p}$	Pressure	$\boldsymbol{T}$	Temperature	$\boldsymbol{K}$	Permeability	$\boldsymbol{\Lambda}$	Thermal cond.

Governing equations and discretization

Finite volumes in space, implicit backward Euler in time

$$\boldsymbol{R}_h^{n+1} = \frac{1}{\Delta t^n}\left([\boldsymbol{M}_w \boldsymbol{u}_w + \boldsymbol{M}_r \boldsymbol{u}_r]^{n+1} - [\boldsymbol{M}_w \boldsymbol{u}_w + \boldsymbol{M}_r \boldsymbol{u}_r]^{n}\right) + \mathtt{div}\left([\boldsymbol{V}_w \boldsymbol{h}_w + \boldsymbol{H}_c]^{n+1}\right) - [\boldsymbol{Q}_w \boldsymbol{h}_w]^{n+1} - \boldsymbol{Q}_h^{n+1} = \boldsymbol{0}$$

Conservation of energy

$$\boldsymbol{H}_c = -(\boldsymbol{\Theta}_{hw} + \boldsymbol{\Theta}_{hr})\mathtt{grad}(\boldsymbol{T})$$

Fourier's law

- Conductive heat flux $\boldsymbol{H}_c$ discretized by two-point method (same as mass flux)
  - $(\boldsymbol{\Theta}_{hw} + \boldsymbol{\Theta}_{hr})\mathtt{grad}$: discrete representation of $(\boldsymbol{\Lambda}_w + \boldsymbol{\Lambda}_r)\nabla$
  - $\boldsymbol{\Theta}_{hw}$, $\boldsymbol{\Theta}_{hr}$: vectors of interface heat transmissibilities

$\boldsymbol{M}$	Mass	$\boldsymbol{V}$	Flux	$\boldsymbol{Q}$	Sources/sinks	g	Gravity
$\boldsymbol{\rho}$	Density	$\boldsymbol{\mu}$	Viscosity	$\boldsymbol{u}$	Internal energy	$\boldsymbol{h}$	Enthalpy
$\boldsymbol{p}$	Pressure	$\boldsymbol{T}$	Temperature	$\boldsymbol{K}$	Permeability	$\boldsymbol{\Lambda}$	Thermal cond.

Case 1: Storage in conceptual five-spot pattern

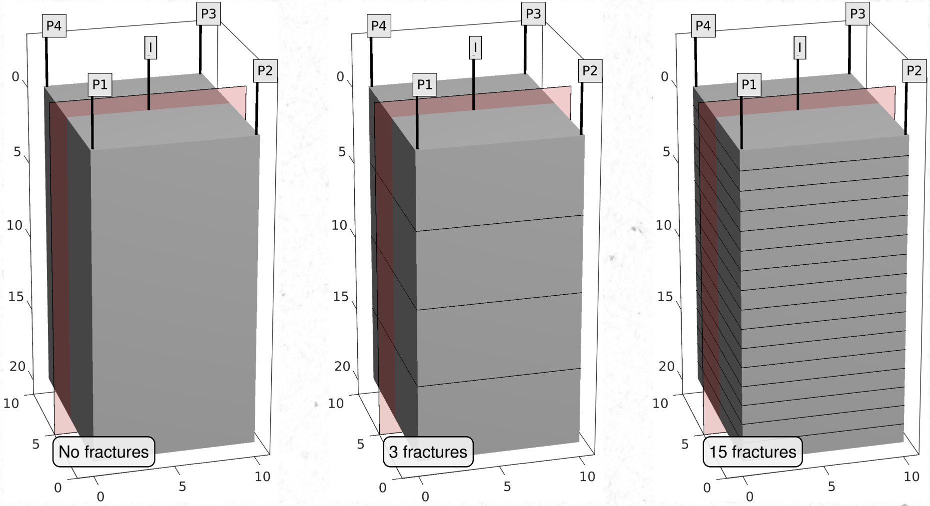

Case 1: Storage in conceptual five-spot pattern

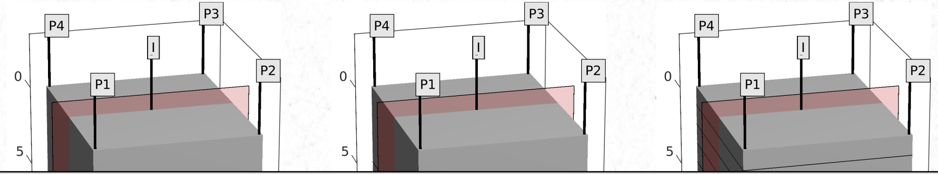

- Box-shaped domain with one well in the center and one well in each corner
- Charging: hot water injected through center well at fixed rate, corner wells produce at fixed BHP
- Discharging: hot water extracted through center well and reinjected in corners after heat is extracted
- Compare effect of 3 vs. 15 fractures and 1 mm vs. 3 mm aperture

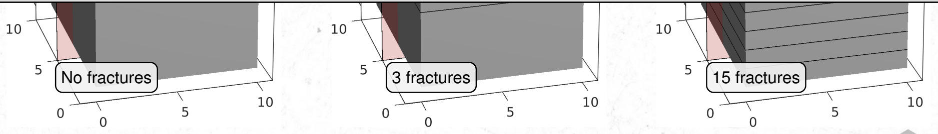

Case 1: Storage in conceptual five-spot pattern

Upscaled, homogeneous perm/poro

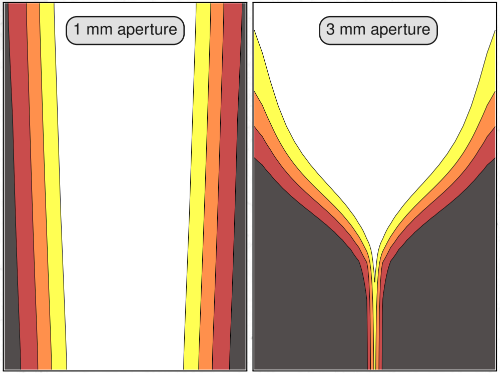

3 fractures

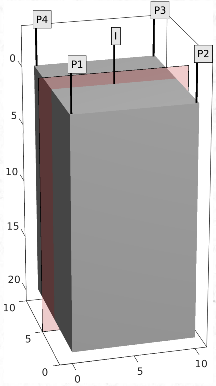

Temperature at red cross-section

Case 1: Storage in conceptual five-spot pattern

Upscaled, homogeneous perm/poro

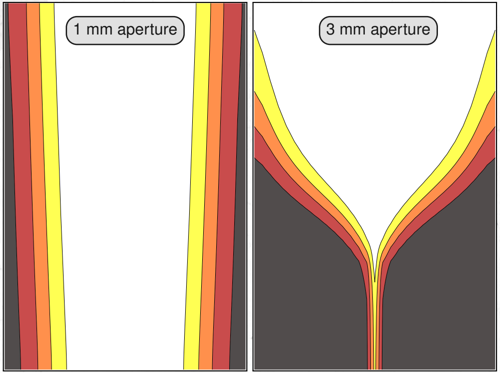

3 fractures

Piston-like heat displacement

→ reasonable pressure buildup, but gross overestimation of stored energy

Case 1: Storage in conceptual five-spot pattern

Upscaled, homogeneous perm/poro

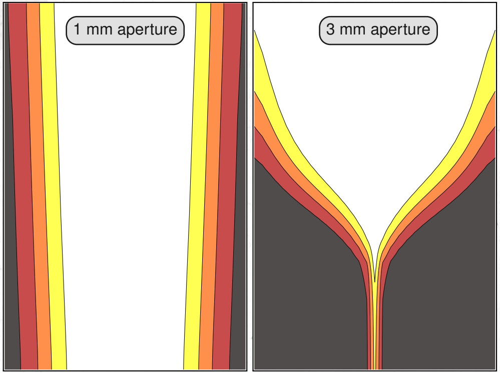

3 fractures

Piston-like heat displacement
→ reasonable pressure buildup, but gross overestimation of stored energy

Solution: explicitly represent fractures with *discrete fracture model* (DFM) (Karimi-Fard, Durlofsky, and Aziz 2004)

Case 1: Storage in conceptual five-spot pattern

Upscaled, homogeneous perm/poro

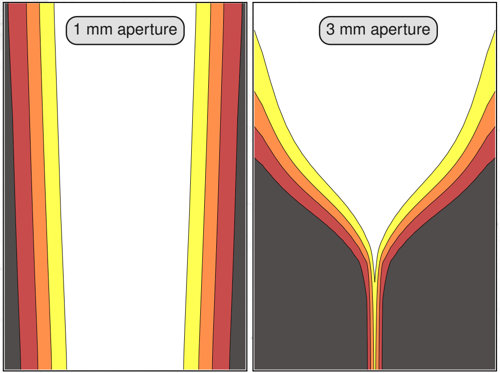

3 fractures

Discrete fracture model

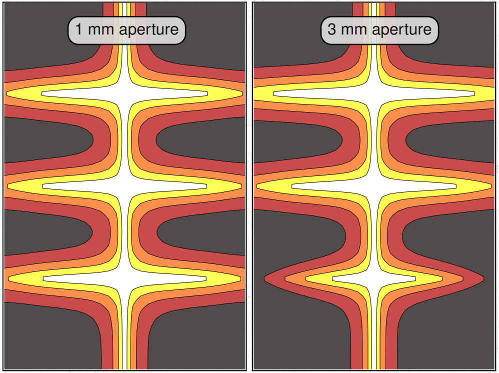

3 fractures

Case 1: Storage in conceptual five-spot pattern

Upscaled, homogeneous perm/poro

Discrete fracture model

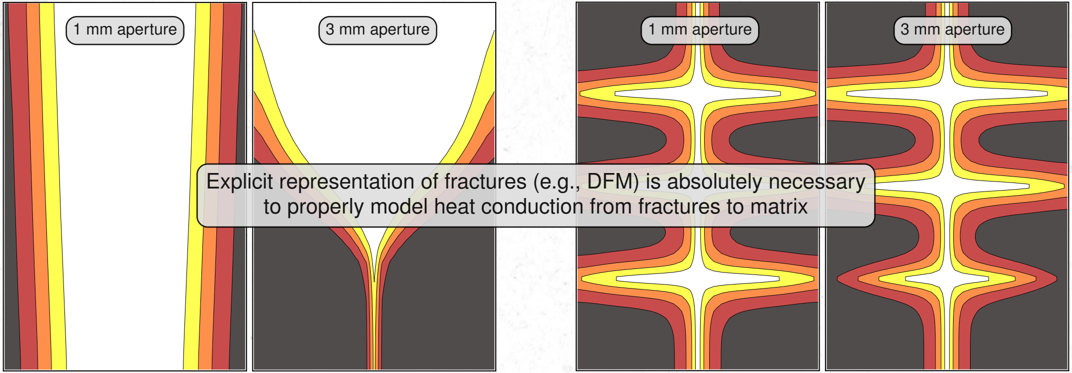

3 fractures

3 fractures

Explicit representation of fractures (e.g., DFM) is absolutely necessary to properly model heat conduction from fractures to matrix

Case 1: Storage in conceptual five-spot pattern

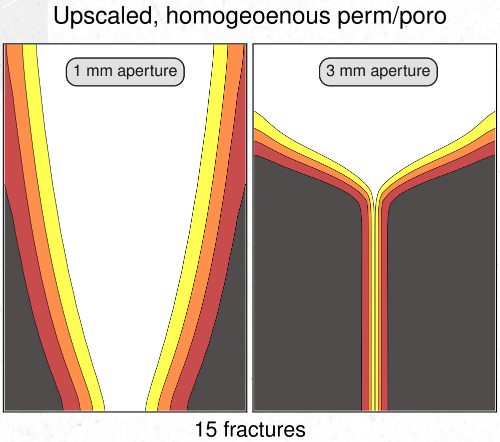

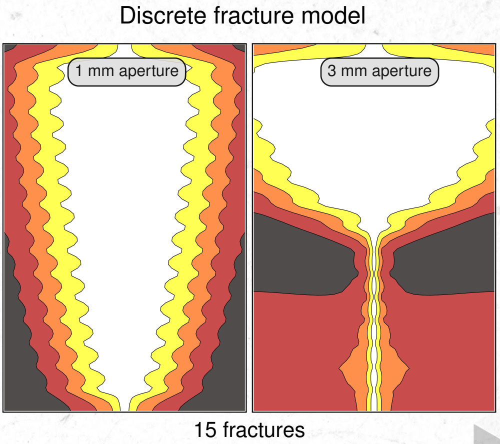

Case 1: Storage in conceptual five-spot pattern

Short inter-well distance, low pressure differences, significant buoyancy effects → unresolved wellbore flow leads to non-physical flow pattern

Solution: full wellbore model with *conservation of mass/energy*

Discrete fracture model

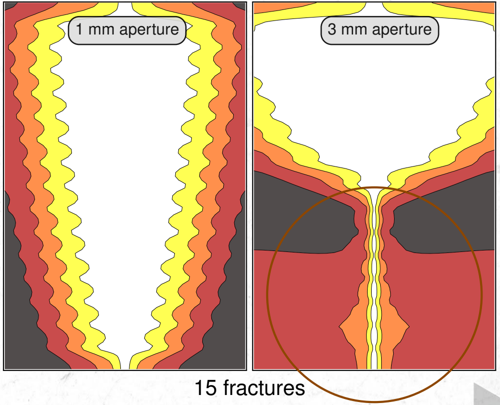

15 fractures

Case 1: Storage in conceptual five-spot pattern

Full well model

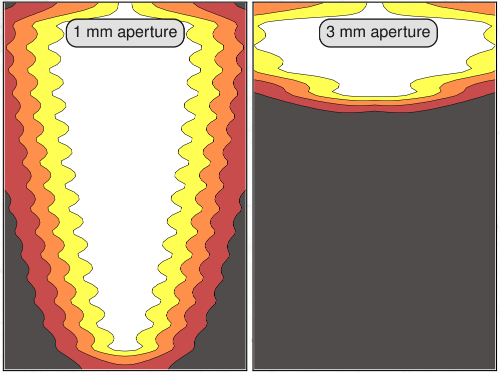

15 fractures

Simple well model

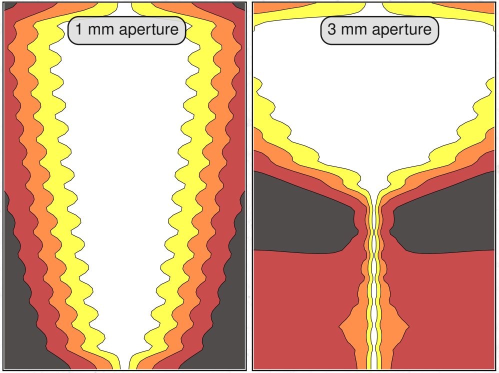

15 fractures

Case 1: Storage in conceptual five-spot pattern

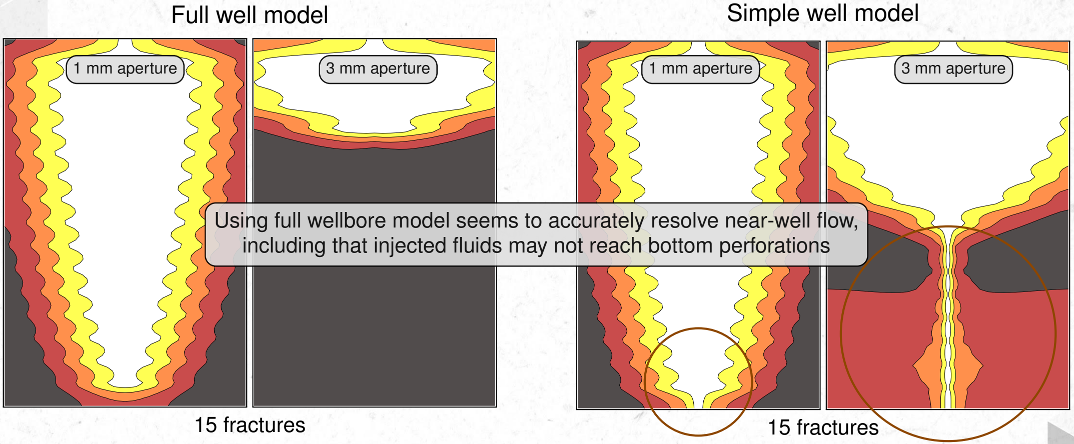

Using full wellbore model seems to accurately resolve near-well flow, including that injected fluids may not reach bottom perforations

Case 1: Storage in conceptual five-spot pattern

Optimal control

- Huge potential in optimizing injection rates and temperatures
- Automatic differentiation enables *gradient-based* optimization
  - Compute Hessian updates by LBFGS algorithm

Gradient-based optimization

Given reservoir states $\boldsymbol{u}^n$, model and/or control parameters $\boldsymbol{m}^n$ and residuals $\boldsymbol{R}^{n+1}(\boldsymbol{u}^n, \boldsymbol{u}^{n+1}, \boldsymbol{m}^{n+1})$, determine parameters $\boldsymbol{m}^n$ that minimizes objective $J(\boldsymbol{u}^{1:N}, \boldsymbol{m}^{1:N})$ using gradients ∇J found by solving *adjoint equations*

Case 1: Storage in conceptual five-spot pattern

Optimal control

- Setup: heat storage in 60 × 60 × 20 m box, homogeneous perm/poro of 2 md/0.04
- Charge for specific time, then discharge to provide peak load to external application
- Objective: find injection rate/temperature that minimizes associated energy costs

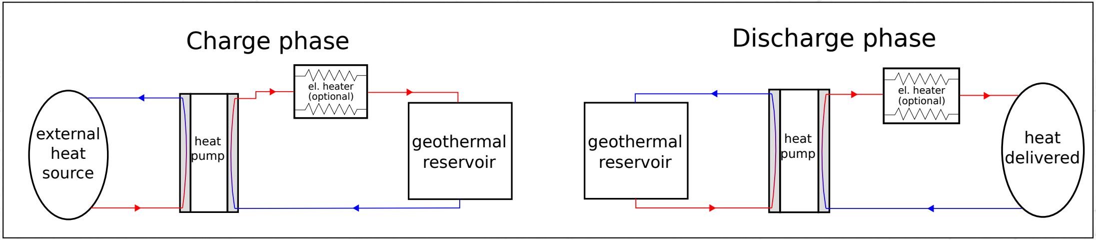

Case 1: Storage in conceptual five-spot pattern

Optimal control – simple and complex scenario

	Simple scenario	Complex scenario
Charge period (days)	30	15
Discharge period (days)	4	4
Energy price (NOK/kWh)	1.5	0.75 - 1.5 - 3.0
Charge: max power from source (MW)	1	1
Discharge: power delivery required (MW)	8	8
Initial reservoir temperature, T_0 (°C)	10	10

Four strategies: no heat storage, base case storage, optimized storage with constant and varying temperature/rate

Case 1: Storage in conceptual five-spot pattern

Optimal control results – complex scenario

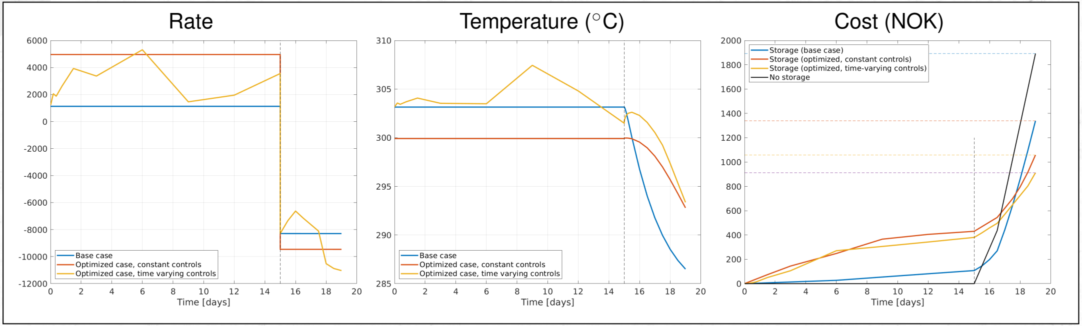

Case 1: Storage in conceptual five-spot pattern

Optimal control results – complex scenario

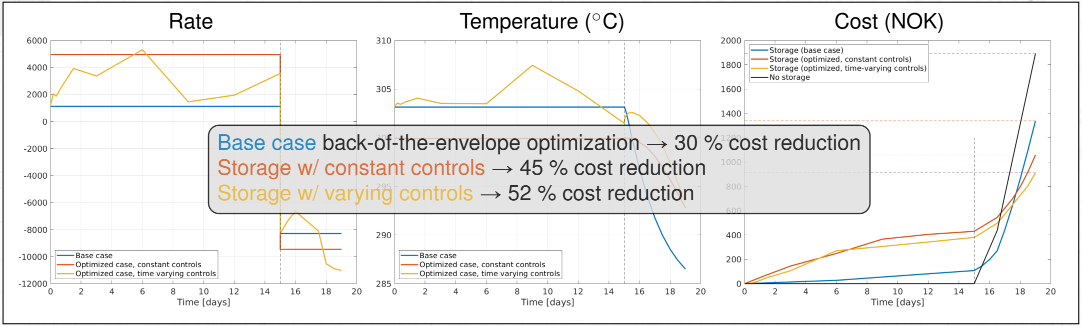

Base case back-of-the-envelope optimization → 30 % cost reduction
Storage w/ constant controls → 45 % cost reduction
Storage w/ varying controls → 52 % cost reduction

Case 1: Storage in conceptual five-spot pattern

Optimal control results – complex scenario

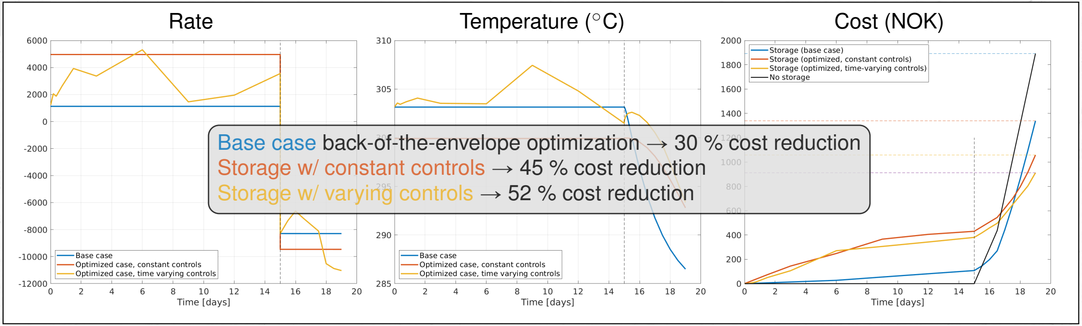

Base case back-of-the-envelope optimization → 30 % cost reduction
Storage w/ constant controls → 45 % cost reduction
Storage w/ varying controls → 52 % cost reduction

*Constantly varying rate/temperature likely not possible – adjusting at given intervals more tractable

EAGE

Case 3: Wesselkvartalet

- Newly constructed, mixed residential/commercial building in the city of Asker, Norway
- Integrates a multi-reservoir, shallow geothermal storage facility for heating/cooling
  - Three reservoirs at different depths with very different properties
  - More than 100 wells, coupled in groups
  - Provides constant base load and rapid release of heat at peak loads
  - Heat energy in the winter to distributed deicing system for the city streets

Case 3: Wesselkvartalet

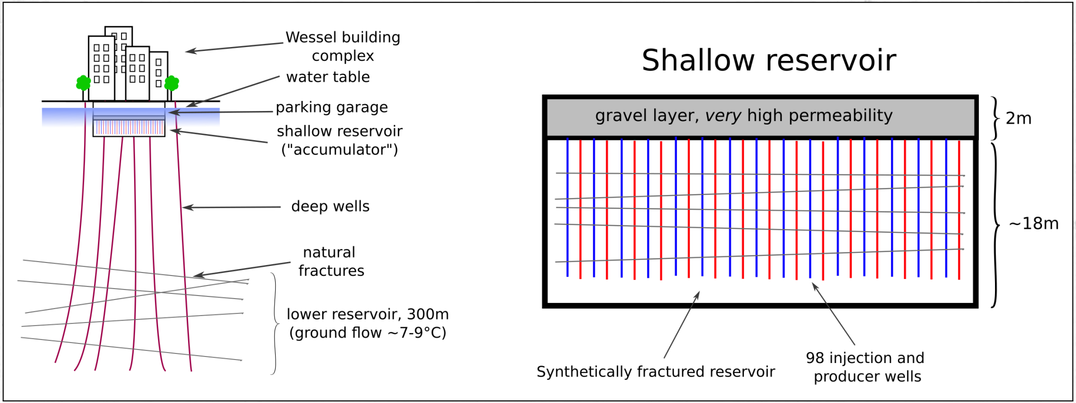

Case 3: Wesselkvartalet

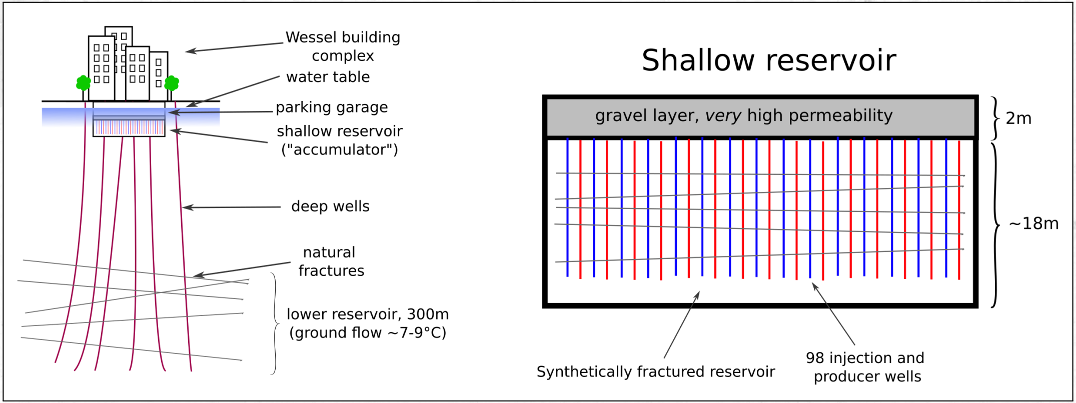

Here: focus on shallow reservoir only

Case 3: Wesselkvartalet – building the model

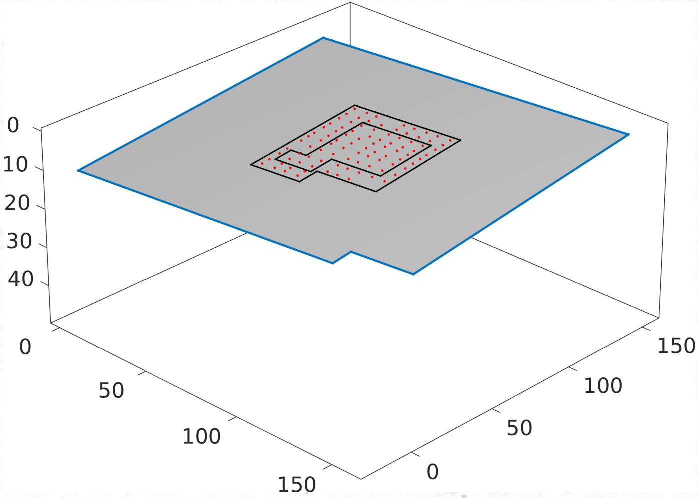

Case 3: Wesselkvartalet – building the model

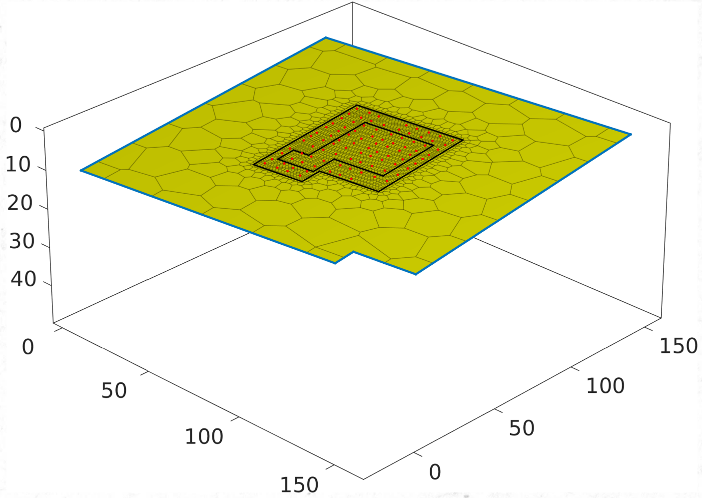

Case 3: Wesselkvartalet – building the model

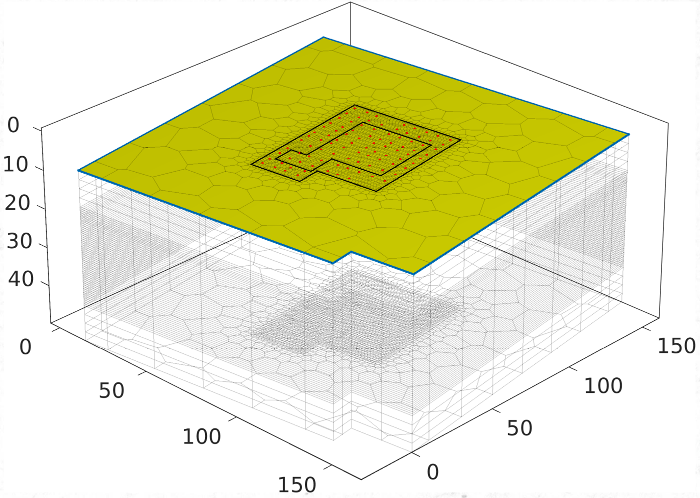

Case 3: Wesselkvartalet – simulation results

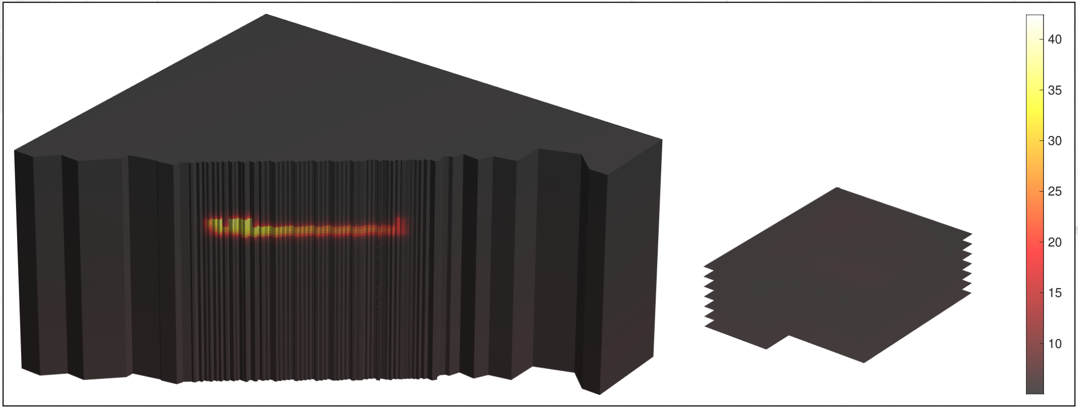

Matrix and fracture temperature (°C), June 28

Case 3: Wesselkvartalet – simulation results

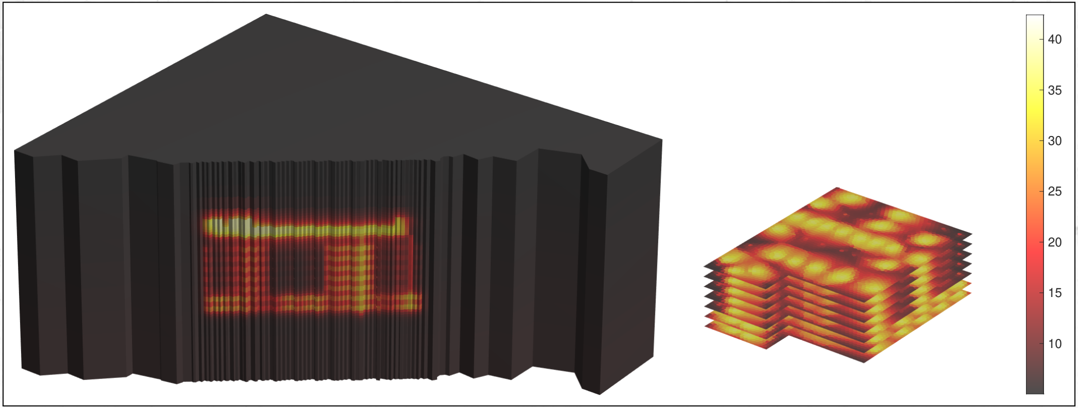

Matrix and fracture temperature (°C), July 22

Case 3: Wesselkvartalet – simulation results

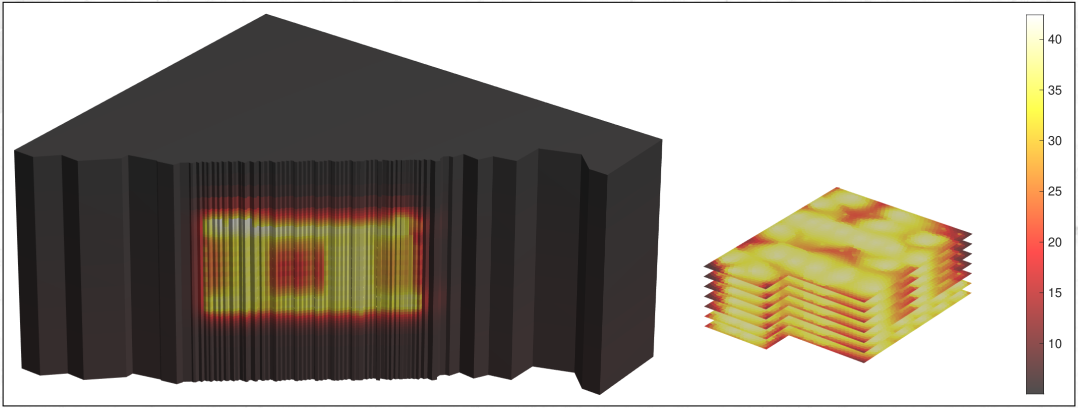

Matrix and fracture temperature (°C), August 28

Case 3: Wesselkvartalet – simulation results

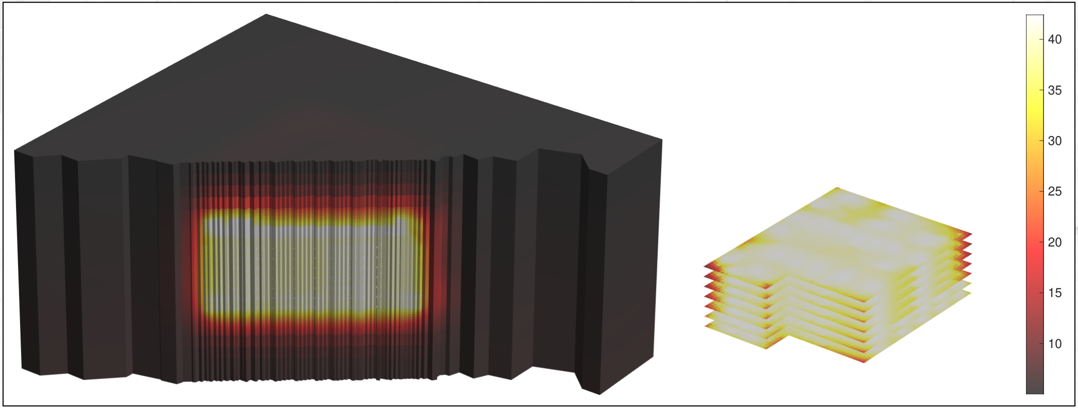

Matrix and fracture temperature (°C), November 21

Case 3: Wesselkvartalet – simulation results

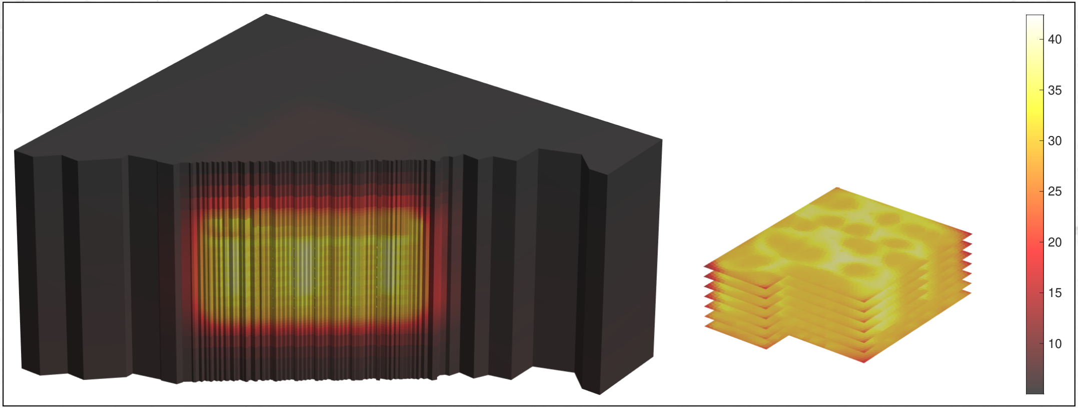

Matrix and fracture temperature (°C), December 15

Case 3: Wesselkvartalet – simulation results

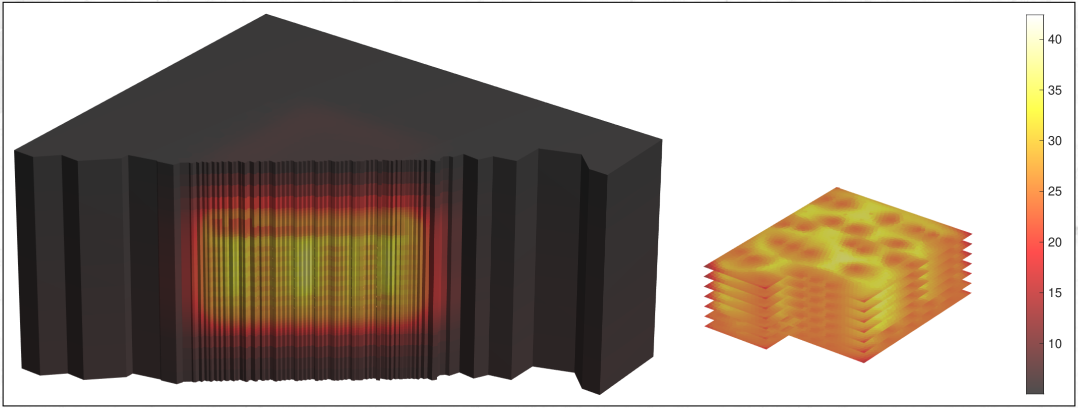

Matrix and fracture temperature (°C), January 8

Case 3: Wesselkvartalet – simulation results

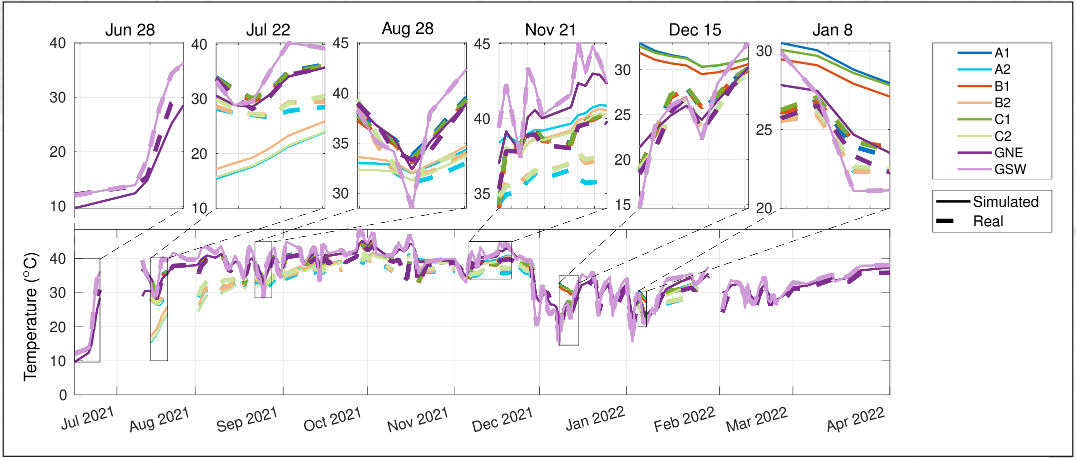

Case 3: Wesselkvartalet – simulation results

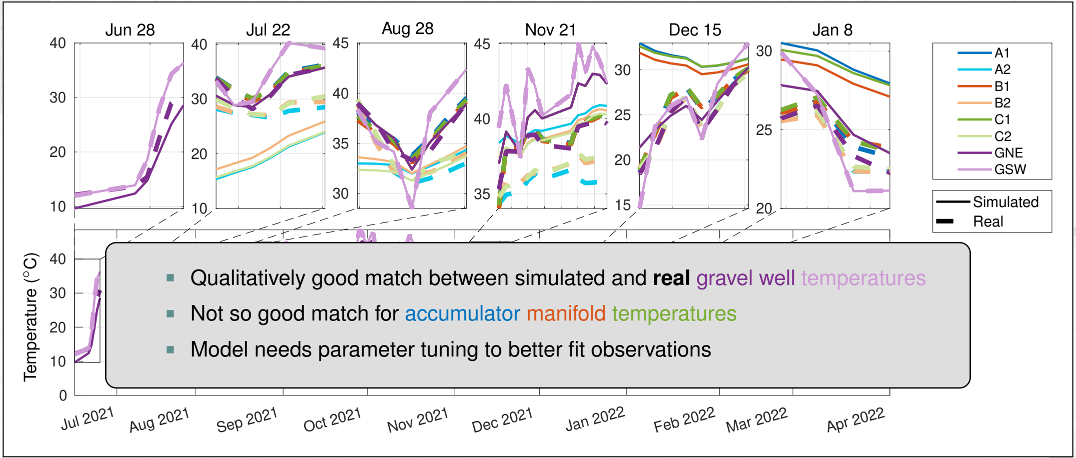

- Qualitatively good match between simulated and **real** gravel well temperatures
- Not so good match for accumulator manifold temperatures
- Model needs parameter tuning to better fit observations

Case 3: Wesselkvartalet – model tuning

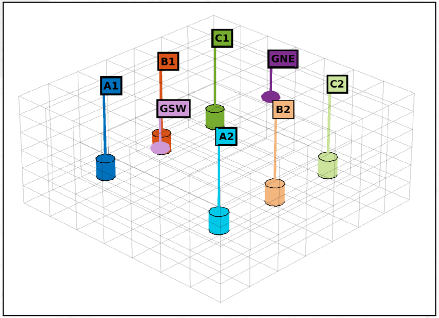

Coarse network model

- Use gradient-based optimization with manifold temperature mismatch as objective
  - Recast as nonlinear least-squares problem → use Levenberg Marquardt algorithm
- Tune *coarse-grid network model* with manifolds only instead of full model w/ 97 wells
  - CGNet (Lie and Krogstad 2021, submitted)
- Parameters tuned: pore volumes, flow/thermal transmissibilities, heat capacities

Case 3: Wesselkvartalet – model tuning

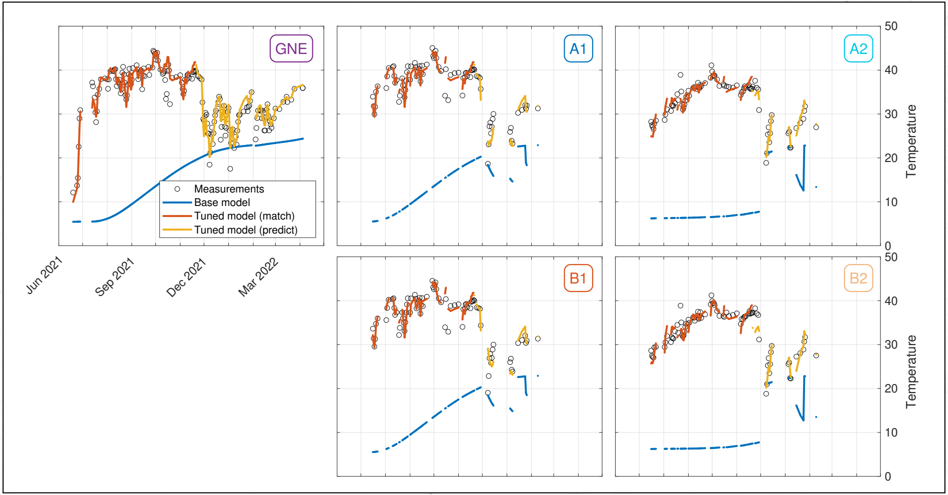

Case 3: Wesselkvartalet – model tuning

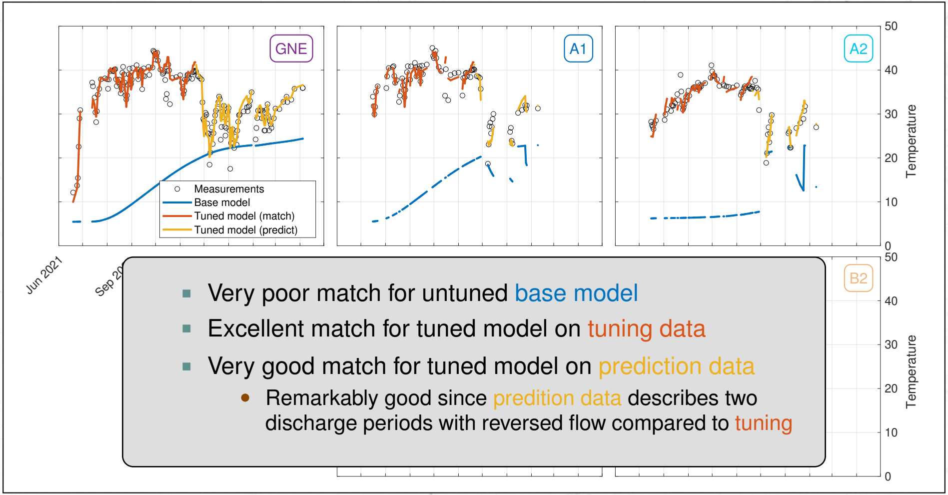

- Very poor match for untuned base model
- Excellent match for tuned model on tuning data
- Very good match for tuned model on prediction data
  - Remarkably good since predition data describes two discharge periods with reversed flow compared to tuning

EAGE

Concluding remarks

Conclusions

- Integrated framework for modelling and optimization of geothermal heat storage
  - Based on methods from simulation of oil and gas reservoirs
  - Fracture mass and heat flow (DFM), accurate wellbore modelling
  - Gradient-based optimization capable of optimal control and parameter tuning
- Simplified parameter study highlights important modelling aspects
  - Explicit fracture modelling is important when the rock is sparsely fractured
  - Densely fractured plants may be adequately modelled using upscaled rock parameters
  - Modelling mass/heat flow inside wellbore has significant effect on simulated performace

Concluding remarks

Further work

- Full wellbore model yields physically reasonable results, but reamins to be validated
- Extreme aspect ratios and distinctly different flow regimes leads to poor convergence
  - Research efficient linear and nonlinear solution strategies (domain/variable decomposition, linear/nonlinear preconditioners, etc.)
- Model parameter tuning has only been tested for very simplified model
  - Open question: can this be used to infer physical properties of underlying system?

EAGE

Acknowledgements

The authors would like to thank Ruden AS, Wessel Energy AS, and Kvitebjørn Varme AS for allowing the publication of this work

EAGE

Case 3: Wesselkvartalet (extra) – operation

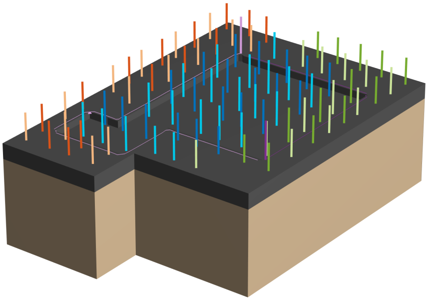

Gravel layer and accumulator

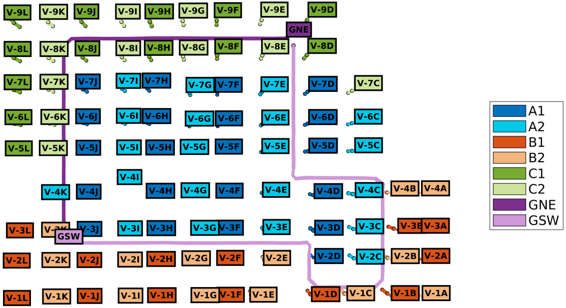

Wells (from above)

Charge

Gravel layer	↓ HP → GSW → GNE ↑
Gravel layer + accumulator	↓ HP → GSW → GNE → (A1,B1,C1) → (A2,B2,C2) ↑

Case 3: Wesselkvartalet (extra) – operation

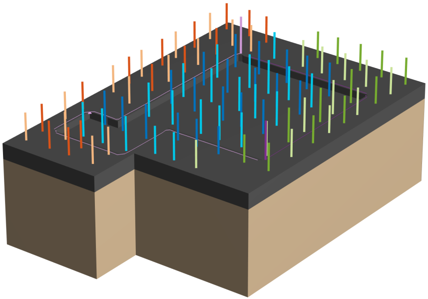

Gravel layer and accumulator

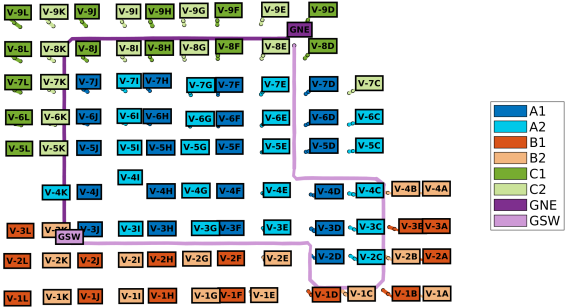

Wells (from above)

Discharge	Gravel layer	↓ GSW → GNE → HP ↑
	Gravel layer + accumulator	↓ GSW → GNE → (A2,B2,C2) → (A1,B1,C1) → HP ↑

Case 2: District heating in Tromsø

- Pilot plant for storage of excess heat from waste incineration under development
  - Buffer imbalance: constant energy supply (waste) and seasonal/daily variations in demand
- Complex geology with large number of natural fractures, some filled with clay
- Fist phase: one injection well circled by seven to eight production wells
  - 300 m deep, fractures/pores cemented first 50 m to minimize heat loss
  - Goal: store approximately 20 GWh/year, deliver more than 10 GWh/year
  - Plan: enhance flow by combination of fracture stimulation and hydraulic fracturing

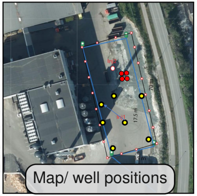
Map/ well positions

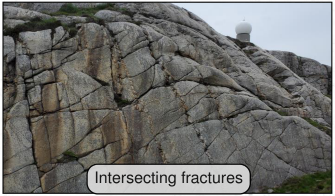
Intersecting fractures


Clay-filled fault

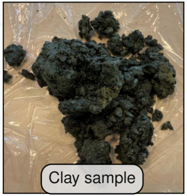
Clay sample

EAGE

Case 2: District heating in Tromsø

- Pilot plant for storage of excess heat from waste incineration under development
  - Buffer imbalance: constant energy supply (waste) and seasonal/daily variations in demand
- Complex geology with large number of natural fractures, some filled with clay
- Fist phase: one injection well circled by seven to eight production wells
  - 300 m deep, fractures/pores cemented first 50 m to minimize heat loss
  - Goal: store approximately 20 GWh/year, deliver more than 10 GWh/year
  - Plan: enhance flow by combination of fracture stimulation and hydraulic fracturing

Herein: preliminary numerical study assessing to what extent the reservoir needs to be fractured/stimulated to achieve this

Case 2: District heating in Tromsø

Model construction: Conforming 2D Voronoi grid extruded vertically

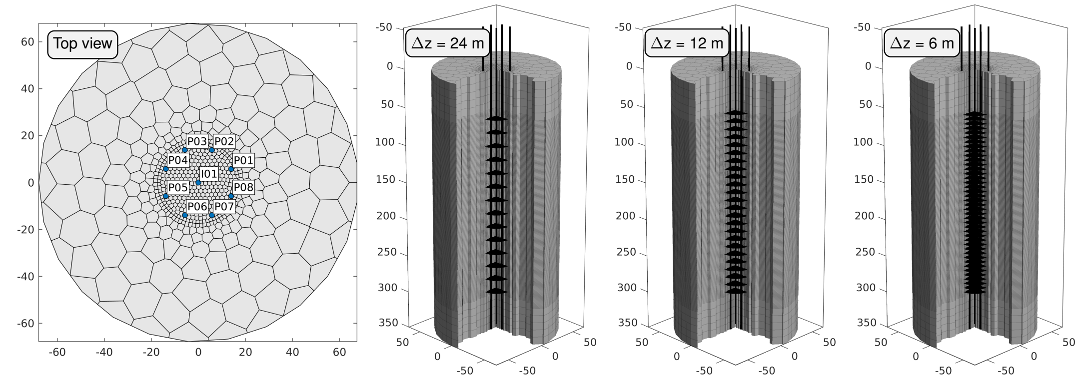

Case 2: District heating in Tromsø

Model construction: Conforming 2D Voronoi grid extruded vertically

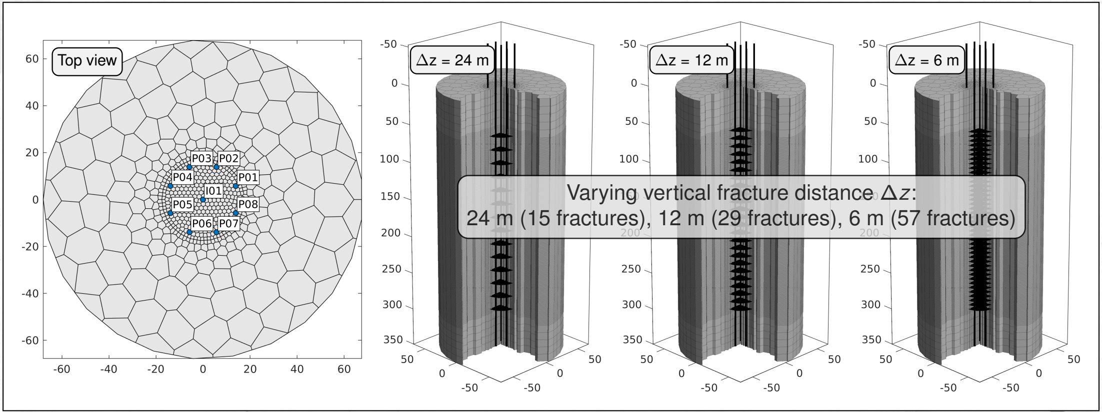

Case 2: District heating in Tromsø

Simulation results: Matrix temperature after 6 months of charging

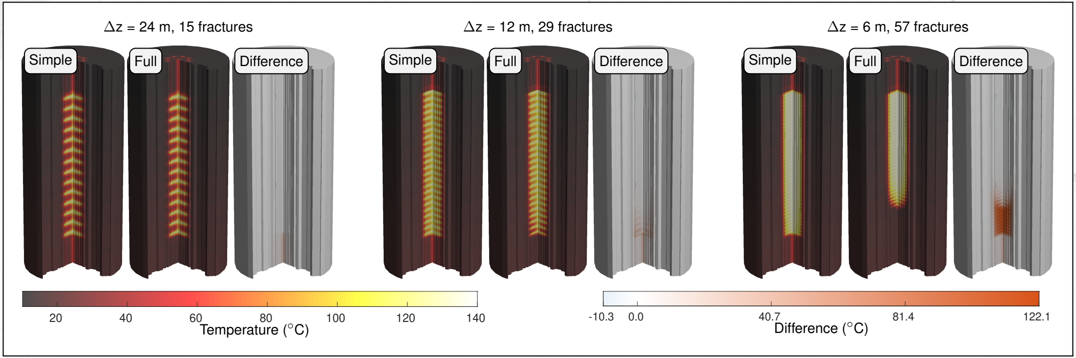

Case 2: District heating in Tromsø

Simulation results: Matrix temperature after 6 months of charging

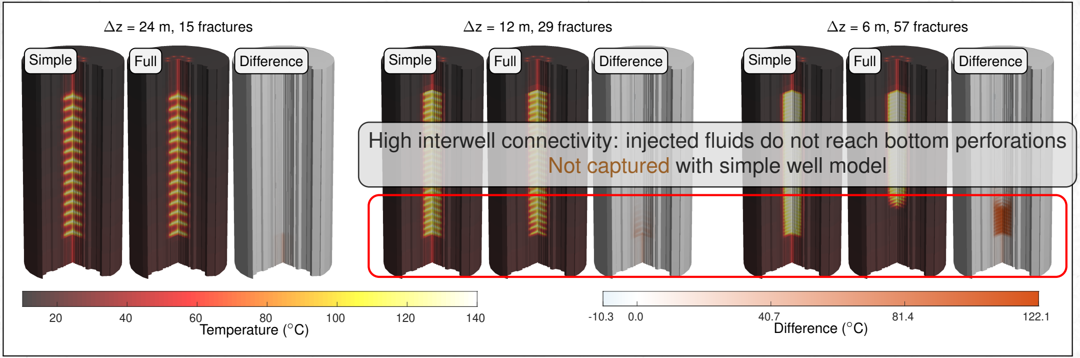

Case 2: District heating in Tromsø

Simulation results: Matrix temperature after 6 months of discharging

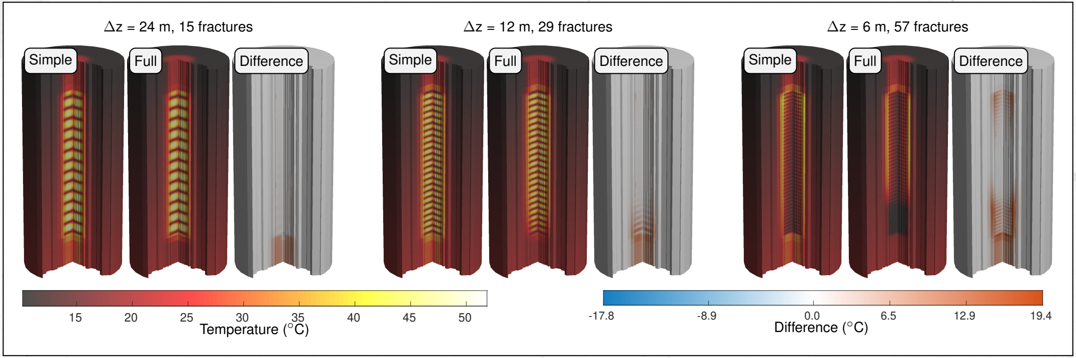

Case 2: District heating in Tromsø

Simulation results: Matrix temperature after 6 months of discharging

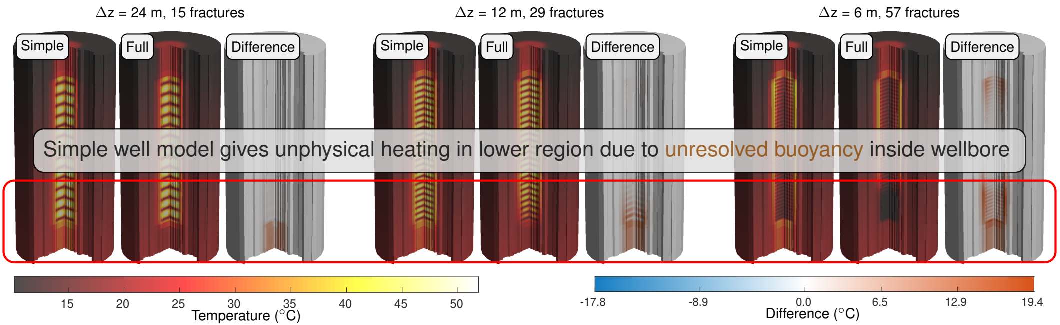

Case 2: District heating in Tromsø

Simulation results: Cumulative stored and produced energy vs. time

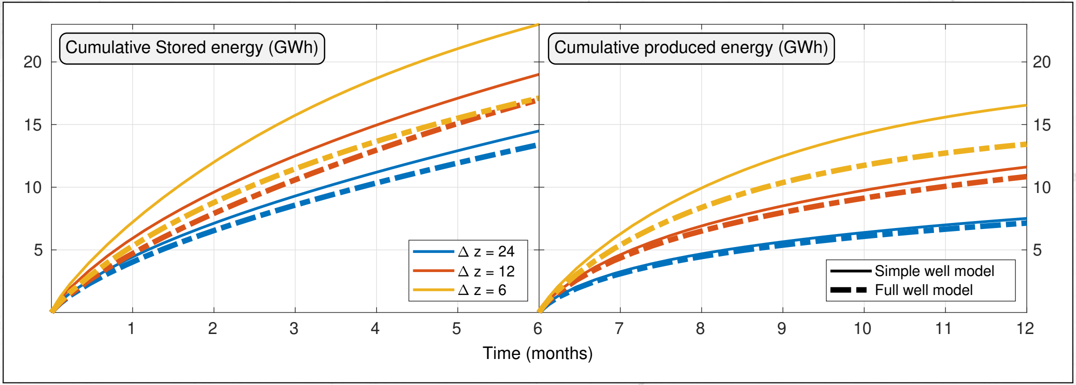

EAGE

Case 2: District heating in Tromsø

Bouyancy effects renders parts of reservoir unused

- More stored energy for $\Delta z = 12$ m
- ... but larger recovery factor for $\Delta z = 6$ m
- May look different after multiple cycles

Simulation results: Cumulative stor